RSC Advances

ROYAL SOCIETY OF CHEMISTRY

www.rsc.org/advances

Aptamer density dependent cellular uptake of lipid-capped polymer nanoparticles for polyvalent targeted delivery of vinorelbine to cancer cells

Zhenbao Liu[a], Huanzhe Zhao[a], Lingyun He[a], Yao Yao[a], Yanbin Zhou[a], Jianping Wu[a], Juewen Liu[a.b.]*, Jinsong Ding [a.]*

[a] *School of Pharmaceutical Sciences, Central South University, Changsha 410013, Hunan Province, People's Republic of China*

[b] *Department of Chemistry, Waterloo Institute for Nanotechnology, University of Waterloo, Waterloo, Ontario, Canada, N2L 3G1*

* Corresponding author

Juewen Liu

Email: liujw@uwaterloo.ca

Telephone: 519-888-4567 ext. 38919

Fax: (519) 746-0435

Jinsong Ding

Email:dingjs0221@163.com

Telephone: 86-731-82650250

Fax: (86)-731-82650442

Abstract

In this work, MUC1 aptamer (designated S2.2) modified and vinorelbine (VRL) loaded lipid-polymer hybrid nanoparticles (Apt-VRL-NPs) were prepared. Their cancer cell targeting efficiency and cell growth inhibition activity were investigated. The S2.2 aptamer was covalently linked to 1,2-distearoyl-sn-glycero-3-phosphoethanolamine-N-carboxy(polyethylene glycol)2000 (DSPE-PEG_{2000}-COOH) using EDC/NHS coupling to obtain a DSPE-PEG2000-Apt conjugate. The nanoparticles were then fabricated by a self-assembly method, using poly lactic-co-glycolic acid (PLGA) as the core and lipids (lecithin and DSPE-PEG_{2000}-COOH and DSPE-PEG_{2000}-Apt) as the shell. By adjusting the molar ratio of DSPE-PEG_{2000}-Apt conjugate to total DSPE materials (DSPE-PEG_{2000}-Apt and DSPE-PEG_{2000}-COOH), nanoparticles with different aptamer densities were obtained. Transmission electron microscopy (TEM) indicates that the particles are spherical. Dynamic light scattering (DLS) measures the average diameter to be below 170 nm and zeta-potential to be around -30 mV. The VRL encapsulation efficiency was between 50% and 60%. The accumulative VRL released into PBS (pH 7.4) over 108 h was lower than 50%, indicating a sustained release characteristic. The nanoparticle uptake efficiency was significantly higher in MUC1 overexpressing breast cancer cells (MCF-7) than in MUC1 negative cells (HepG2) as demonstrated by fluorescence microscopy and by quantitative fluorescence measurement. The MCF-7 cell targeting efficiency is enhanced with increased density of the S2.2 aptamer. The *in vitro* cell inhibition study shows enhanced toxicity of S2.2-modified nanoparticles.

Keywords: Hybrid nanoparticles; Aptamers; MUC1; Tumor targeting; Ligand density

Introduction

Amongst the various types of drug delivery vehicles developed for cancer therapy, lipid-based materials are highly attractive for their excellent biocompatibility.[1-3] Currently, a large fraction of approved nanoscale drug carriers are made of lipids.[4] Traditional liposomal vehicles however suffer from low drug encapsulation efficiency, low stability, and spontaneous lysis.[5] Over the past decade, a number of advances have been made to improve on these aspects. For example, inorganic nanoparticle (NP) cores have been employed to adsorb drugs and prepare supported bilayers.[6-12] While the drug loading aspect has been improved, the potential toxicity of inorganic materials has lessened the benefit of lipids. An alternative approach is to employ a biocompatible polymeric core. Polymer NPs have a relatively high encapsulation efficiency and drug release is also more controllable. The combination of lipid and polymer takes advantage of the properties of both materials.[13-21] The diameter of nanoparticles can be controlled by adjusting the lipid/polymer ratio.[22] The lipid shell can also retard the permeation of water into the core of the NPs, slowing down core degradation and allowing sustained release over a longer period of time.[23] Since most anti-cancer drugs are quite hydrophobic, the polymer cores are often hydrophobic as well, supporting lipid monolayers instead of bilayers.

To go from passive to active delivery, a targeting ligand needs to be grafted on the particle surface.[24-26] Common targeting ligands include antibodies, peptides, aptamers and small molecules, which can specifically target proteins that are overexpressed on cancer cells.[16,27-31] Aptamers are single-stranded DNA or RNA that can selectively bind to various target molecules. With the development of cell SELEX (i.e. using live cells as targets), many new aptamers have been isolated for a broad range of cancer cell lines.[32-35] Aptamers, especially DNA aptamers, have higher stability and lower immunogenicity as compared to antibodies.[36,37] Aptamers are also smaller, facilitating penetration into solid tumors as well as in vivo cellular uptake. Due to their excellent target binding property and ease of modification, aptamers have been conjugated to many types of nanomaterials for targeted delivery.[38-40]

In this study, we chose an MUC1 aptamer named S2.2 as the targeting molecule. This aptamer was first developed by Ferreira *et al.* to target the MUC1 protein.[41] MUC1 is a large transmembrane glycoprotein, which is ~10-fold overexpressed in most malignant tumors including ovarian, lung, pancreatic, prostate, and breast cancers. S2.2 is a 25-nucleotide truncated version of the original aptamer. It binds MUC1 with high specificity and affinity

(K_d = 0.135 nM). S2.2 has been used in a few targeted delivery systems with polymer and metallic nanoparticles,[42-45] but it has not been studied in polymer/lipid systems. Lipid sealed polymers minimize polymer hydrolysis and are more biocompatible than inorganic metallic nanoparticles.

Vinorelbine (VRL) is a semi-synthetic vinca alkaloid chemotherapy drug for treating many types of cancer, such as non-small cell lung cancer,[46] and advanced and metastatic breast cancer through inhibiting mitosis.[47] However, VRL has a number of issues when directly administered intravenously, including venous irritation, phlebitis, and toxicity to normal cells. Therefore, delivery strategies are needed to encapsulate VRL. VRL is poorly soluble in water. Previous studies showed that solid lipid nanoparticles can entrap VRL with about 80% efficiency.[48] We recently used PLGA NPs for loading VRL.[49] In this study, we constructed an S2.2-conjugated lipid-polymer NP for delivery of VRL to MUC1-positive cancer cells. In particular, our synthesis method allows us to systematically evaluate the density of aptamer on the particle surface.

Materials and Methods

Chemicals. Vinorelbine (VRL, Batch No: 20110901, purity>99%) was purchased from Hainan Yueyang Biotech Co., Ltd (Hainan, China). 3′ amino-modified S2.2 DNA aptamer with sequence of 5′ GCAGTTGATCCTTTGGATACCCTGG-NH_2 3′ was obtained from Sangon Biotech (Shanghai, China). 1,2-distearoyl-sn-glycero-3-phosphoethanolamine-N-carboxy(polyethylene glycol)$_{2000}$ (DSPE-PEG_{2000}-COOH), Poly (lactic-co-glycolic acid) (PLGA) (50/50, MW = 15,000) was from Jinan Daigang Biomaterial Co., Ltd (Jinan, China). DSPE-PEG_{2000}-COOH was from NANOCS (USA). Lecithin was from Lipoid (Germany). Acetonitrile was from TEDIA (Arizona, USA). Methanol, ethanol, phosphate buffer saline (0.01 M, pH7.4) and dimethyl sulfoxide (DMSO) were from Sinopharm Chemical Reagent Co., Ltd (Beijing, China). Ammonium acetate, triethylamine, acetic acid, $NaH_2PO_4 \cdot 2H_2O$, $Na_2HPO_4 \cdot 12H_2O$, *N*-(3-dimethylaminopropyl)-*N*′-ethylcarbodiimide hydrochloride (EDC·HCl), *N*-hydroxysuccinimide (NHS), coumarin 6 (cou-6), and 3-(4,5-Dimethylthiazol-2-yl)-2,5-diphenyltetrazolium bromide (MTT) were provided by

Sigma-Aldrich (St. Louis, MO, USA). 2-(4-Morpholino) ethane sulfonic acid (MES) and trypsin were obtained from Beijing Dingguo Changsheng Biotechnology CO. LTD (Beijing, China). DMEM medium with high glucose was purchased from GIBCO (Grand Island, NY, USA). Penicillin streptomycin combination (100×), Fetal Bovine Serum (FBS), Hank's buffer (HBSS), paraformaldehyde, Tween 20, Glycine, and 4',6-diamidino-2-phenylindole (DAPI) were from Solarbio (Beijing, China). Human liver cancer cell line (HepG2), human breast cancer cell line (MCF-7) were obtained from American Type Culture Collection (Manassas, VA).

Construction of VRL-loaded NPs (VRL-NPs). VRL-NPs were prepared by the self-assembled method[50] using PLGA, lecithin and DSPE-PEG_{2000}-COOH as carrier materials, and VRL as a model anti-cancer drug. DSPE-PEG_{2000}-COOH (0.72 mg) and lecithin (0.48 mg) (3:2, *w/w*) were dissolved in 2 mL ethanol (4%) to prepare the stock solution (0.6 $mg \cdot mL^{-1}$) as aqueous phase. 1.2 mg VRL and 8 mg PLGA (15:100, *w/w*) were dissolved in 1 mL acetonitrile as the organic phase. The water phase was heated to 65 ºC and then the organic phase was added in a drop-wise manner into the water phase with magnetic stirring. The mixture was vortexed for 3 min to promote self-assembly of the NPs. The resulting NPs were dialyzed to remove acetonitrile and non-encapsulated VRL.

Encapsulation efficiency and drug loading efficiency. Equal amounts of sample before and after dialysis were added with equal amount of methanol and ultrasonicated for 30 min to disintegrate the NPs. The concentration of VRL was measured with HPLC using an ODS C_{18} (250 mm×4.6 mm, 5 μm) column. Acetonitrile and ammonium acetate in a 1:1 ratio was chosen as the mobile phase (10 $mmol \cdot L^{-1}$ ammonium acetate, 0.2% triethylamine, pH was adjusted to 4 by glacial acetic acid). Detection wavelength was set at 269 nm, flow rate 1 $mL \cdot min^{-1}$, temperature 40 °C, and injection volume 20 μL. The encapsulation efficiency (EE) and drug loading efficiency (DL) were calculated with the following equation:

EE (%) = (Amount of VRL in the NPs / Amount of VRL used in the formulation)×100%

DL (%) = (Amount of VRL in the NPs / Amount of carrier materials)×100%

Construction of aptamer conjugated and VRL-loaded lipid-polymer hybrid NPs (Apt-VRL-NPs). The 3′ amino-modified S2.2 aptamer was conjugated with DSPE-PEG_{2000}-COOH using EDC·HCl and NHS as coupling agents following literature procedure.[51] Briefly, DSPE-PEG_{2000}-COOH was dissolved in 0.1 M MES buffer (pH 6.0) containing 400 mM of EDC·HCl and 60 mM of NHS. After 30 min, the aptamer was added

and the pH was adjusted to 7.4 with PBS. The reaction was continued in the dark for 2 h under stirring conditions (the molar ratio of aptamer: DSPE-PEG_{2000}-COOH was 10:9). The reactant was transferred into an ultrafiltration tube (MWCO: 10 KD) and centrifuged at 3000 rpm for 20 min. The filtrate was collected and the absorption was measured at 260 nm. To obtain pure DSPE-PEG_{2000}-Apt, the reactant was washed with water until there was no absorption in the filtrate. The concentration of S2.2 apt was determined by dissolving in PBS buffer (0.1 M, pH 7.4), measuring the UV absorption at 260 nm, and developing a standard curve. To calculate the bonding ratio of S2.2 with DSPE-PEG_{2000}-COOH, the following equation was used:

Bonding ratio (%) = (Amount of S2.2 in the DSPE-PEG_{2000}-Apt / Amount of S2.2 used in the formulation)×100%

Through adjusting the molecular ratio of DSPE-PEG_{2000}-Apt: total DSPE materials, different densities of aptamer were prepared (0.5%, 1%, 2%, 5%, and 10%, molar ratio). The Apt-VRL-NPs prepared were correspondingly marked as $Apt_{0.5}$-VRL-NPs, Apt_1-VRL-NPs, Apt_2-VRL-NPs Apt_5-VRL-NPs, and Apt_{10}-VRL-NPs. Cou-6 loaded NPs (Cou-6-NPs) were prepared in a similar way, except that VRL was replaced with Cou-6 (5 μg). Because the solubility of Cou-6 in water is very low (< 50 $ng \cdot mL^{-1}$), the prepared Cou-6-NPs were dialyzed and further centrifuged at 5000 rpm for 10 min to remove acetonitrile and non-encapsulated Cou-6.

Particle morphology and conjugation characteristic. The morphology and size of the NPs was measured by transmission electron microscopy (TEM). Their diameter, PDI, and zeta-potential were measured by dynamic light scattering (Malvern Zetasizer Nano ZS, UK). The covalent linkage of S2.2 with DSPE-PEG_{2000}-COOH was characterized by X-ray photoelectron spectroscopy (XPS).

***In-vitro* release profile.** The *in vitro* release of VRL was studied by the membrane diffusion method. 1 mL of VRL-NPs or Apt_{10}-VRL-NPs was introduced into a dialysis bag (MWCO: 3400) and then immersed into 100 mL PBS (pH 7.4) release medium in an incubator shaker set at 100 rpm and 37 °C. 1 mL sample was withdraw after 0, 2, 4, 8, 10, 12, 24, 48, 72, and 108 h, and replaced with 1 mL fresh release medium after each sampling. The concentration of VRL was measured by HPLC (Shimadzu LC-20AT, Japan) equipped with a Dikma ODS C_{18} (250 nm×4.6 mm, 5 mm) analytical column (40 °C) and a UV/VIS detector operated at 269 nm. VRL-loaded NPs were dissolved in methanol and ultrasonicated for 20 min prior to injection. The cumulative release percentages of VRL were calculated. To determine leakage

of Cou-6, 1 mL of Cou-6-NPs or Apt_{10}-Cou-6-NPs were dialyzed in 100 mL PBS. Samples were withdrawn at 0, 1, 2, 4, 6, 8, 11, 24 h after dialysis. The concentration of Cou-6 was also measured by the HPLC using a fluorescence detector (RF-10AXL, Japan) operated at λ_{ex}=466 nm, λ_{em}=504 nm. The mobile phase was a mixture of methanol and water (95:5, *v/v*), and the flow rate was 1.0 mL/min.

Cell culture. MCF-7 and HepG2 cells were cultured in a medium containing 10% inactivated FBS penicillin (100 $U \cdot mL^{-1}$) and streptomycin (100$\mu g \cdot mL^{-1}$), in a 37 °C, 5% CO_2 incubator (MCO-15AC, SANYO, Japan).

Cellular uptake of Apt-Cou-6-NPs observed with fluorescence microscopy. HepG2 and MCF-7 cells were collected and seeded in a 24 well plate with 500 μL per well (5×10^4/mL). After incubation for 24 h, the medium was removed and cells were washed with HBSS. Cou-6-NPs and Apt_{10}-Cou-6-NPs were diluted with HBSS to 100 $\mu g \cdot mL^{-1}$ (calculated based on the PLGA content). 300 μL of these NPs were added to each well. After further incubation for 30 min, cells were washed with ice cold PBS 3 times. Then 300 μL of 4% paraformaldehyde was added and incubated with the cells for 15 min to fix the cells. The paraformaldehyde was then removed, 100 μL of DAPI solution (100 ng/mL) was added to stain the nucleic acid for 15 min, and the cells were further washed with PBS 2 times. The fluorescence of the cells was observed with an inverted fluorescence microscope (Olympus IX-71, Japan).

Quantitative cellular uptake studies. HepG2 and MCF-7 cells were seeded in a 96 well plate at a concentration of 5×10^3/ well and cultured for 24 h. Then, the medium was removed, the cells were washed with HBSS, and cells were incubated with 100 μL HBSS for 15 min. Cou-6-NPs and Apt_{10}-Cou-6-NPs were diluted with HBSS to 25, 50, 125, 250 $\mu g \cdot mL^{-1}$ (calculated based on PLGA content). 100 μL of this solution was added to the cells and incubated for 30 min (4 replicates). Then the cells were washed with ice cold PBS three times. 100 μL of cell lysis buffer was added to each well and incubated for 30 min to lyse the cells. The fluorescence was measured by a microplate reader (Tecan Infinite M200, λ_{ex}=466 nm, λ_{em}=504 nm), and the cell uptake content was calculated.

Cell growth inhibition. The cells were seeded and cultured in a 96 well plate as described above. After culturing for 24 h, the medium was removed. NPs, Apt, free VRL, and Apt-VRL-NPs were diluted to 12 $\mu g \cdot mL^{-1}$ (calculated or normalized based on the PLGA

content) and the samples were sterile filtrated through a 0.22 μm millipore filter. 100 μL of each NP was added and further incubated with cells for 24 h. Cells without treatment were set as negative controls. 20 μL MTT (5 $\mu g \cdot mL^{-1}$) was added to each well and incubated for 4 h. The medium was removed and 100 μL of DMSO was added. After 10 min, the absorption was measured by the microplate reader at 490 nm and the cell inhibition ratio was calculated. To study the effect of aptamer density, VRL-NPs, $Apt_{0.5}$-VRL-NPs, Apt_1-VRL-NPs, Apt_2-VRL-NPs, Apt_5-VRL-NPs and Apt_{10}-VRL-NPs were diluted with culture medium to 4, 8, 12, 16, 20, 24 $\mu g \cdot mL^{-1}$ (calculated based on VRL concentration). The samples were filtrated through 0.22 μm filter (Millipore). 100 μL of these solutions was added to each well and further incubated for 24 h. The MTT assay was the same as described above. The cell inhibition ratio and IC_{50} were calculated.

Statistical Analysis

All the experiments were performed in triplicate and data was indicated as mean ± SD. Statistical analysis was calculated according to the Student's t-test and one-way ANOVA analysis. $P < 0.05$ was used as the level of significance.

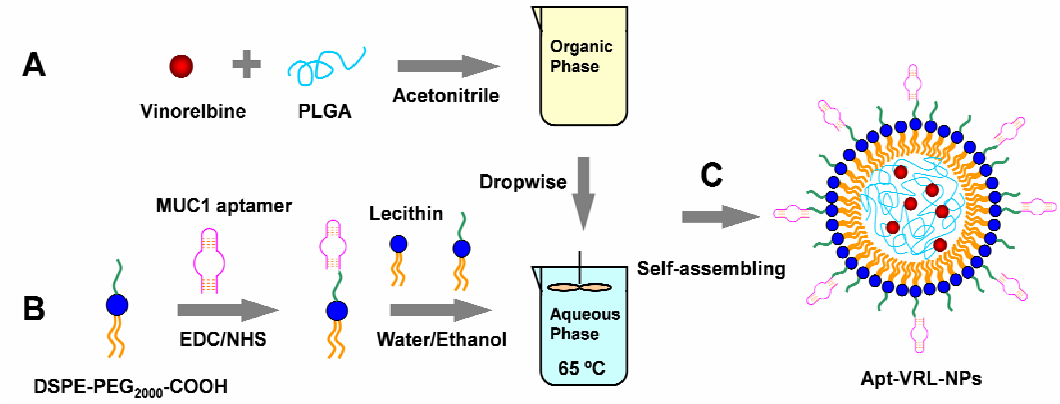

Figure 1. Construction of aptamer conjugated and VRL loaded NPs (Apt-VRL-NPs). (A) VRL and PLGA are dissolved in acetonitrile as the organic phase. (B) Covalent conjugation of the S2.2 aptamer with DSPE-PEG_{2000}-COOH. The conjugate, DSPE-PEG_{2000}-COOH and lecithin are then dissolved in water as the aqueous phase. (C) The organic phase is added dropwise into the aqueous phase at 65 °C under stirring to prepare the NPs by self-assembly.

Results and Discussion

Aptamer-conjugated NPs. The intended structure of our drug delivery system is shown in Figure 1C. It contains a biocompatible and biodegradable PLGA core holding the hydrophobic drug VRL. Compared to liposome encapsulated drugs, the PLGA core significantly retards drug diffusion and enhances encapsulation efficiency.[42] The particle surface is sealed by a lipid monolayer, which serves two functions. First, it protects the internal polymer core from direct contact with water and thus impedes hydrolysis. Second, it provides an anchor for conjugating both polyethylene glycol (PEG) and the aptamer. The PEG chains (molecular weight = 2000) not only provide steric stabilization to increase colloidal stability, but can also reduce protein adsorption.[52-55] In addition, PEG serves as a spacer to increase the flexibility of the aptamer moiety. It has been reported that the binding property of aptamers is often enhanced when they are extended away from the particle surface to reduce steric hindrance.[42,56]

To achieve such a structure, an emulsion synthesis method was employed (Figure 1). Both PLGA and VRL are poorly soluble in water, so they were both dissolved in acetonitrile. Separately, a water/ethanol solution containing three types of lipids was prepared. The majority of the lipids were lecithin, and a small fraction of DSPE-PEG_{2000}-COOH was added (terminated with a carboxyl group). Finally, the amino-labeled aptamer was covalently conjugated to the PEG carboxyl group. Under strong mechanical stirring, the acetonitrile phase was added to the lipid solution in a dropwise manner. Since PLGA is insoluble in the aqueous phase, it self-assembled into NPs, encapsulating VRL, and the surface was also capped by the lipids. In this process, the solution temperature was maintained at 65 °C, such that the lipid chains were above their phase transition temperature to facilitate the self-assembly process. Compared to the traditional liposomal systems, this preparation containing the PLGA core has a higher drug encapsulation efficiency, yet it is simple and controllable.

First, we prepared NPs without the aptamer component (only DSPE-PEG_{2000}-COOH, lecithin and PLGA at 9:6:100, *w/w/w*). The resulting VRL loaded NPs have an average size of 124 nm with a polydispersity index (PDI) of 0.11 as characterized by dynamic light scattering (DLS). Transmission electron microscopy (TEM) indicates that the NPs are spherical (Figure

2A) and the size agrees with that from DLS. The zeta-potential was -27.7 mV in deionized water, which is expected from the carboxyl groups in the PEG chain. The VRL encapsulation efficiency was 50.7%, and the drug loading (by mass) was 6.6%. For comparison, liposomal loading efficiency is typically below 1%. Overall, this is quite an efficient drug loading method.

In the next preparation, the aptamer was incorporated. Two methods are available for aptamer attachment. For example, the NPs prepared above can be used for aptamer conjugation. In our experiment, however, this method led to poor NP stability after the conjugation, which is attributable to the compromised lipid layer integrity during the reaction, leading to aggregation of the polymer core. Therefore, we chose to use a pre-conjugation method (Figure 1), where the aptamer conjugated lipid was part of the synthesis.[57] The aptamer conjugate efficiency was determined to be ~73%.

With this pre-conjugation method, the density of aptamer is readily tunable. Since aptamer density might enhance cellular uptake, we desired to study this effect systematically in this work. A series of NPs were prepared with aptamers ranging from 0 to 10% of the total surface DSPE lipids. Figure 2B shows that the particle size slightly increased from 128 nm to 167 nm with higher aptamer density. Since this aptamer is quite short (see Figure 1 for sequence), the aptamer alone can only extend the particle size by a few nanometers. Therefore, this size increase might be related to a moderate degree of aggregation. Despite the slightly increased size, even the largest formulation is still below 200 nm, which is ideal for drug delivery. If we take 124 nm as the average core size, a 0.5%, 1%, 2%, 5% and 10% molar ratio of Apt-DSPE-PEG_{2000}-COOH loading corresponds to 173, 347, 673, 1732 and 3465 Apt-DSPE-PEG_{2000}-COOH per NP, respectively.

The zeta-potential slightly decreased from -23.7 mV to -32 mV in these NPs (Figure 2C), which could be explained by the increased aptamer density bringing more negative charges to the surface. The encapsulation efficiency of VRL remained quite constant (Figure 2D), indicating the aptamer component did not affect drug loading. This is reasonable since the loaded drug resides only in the PLGA core.

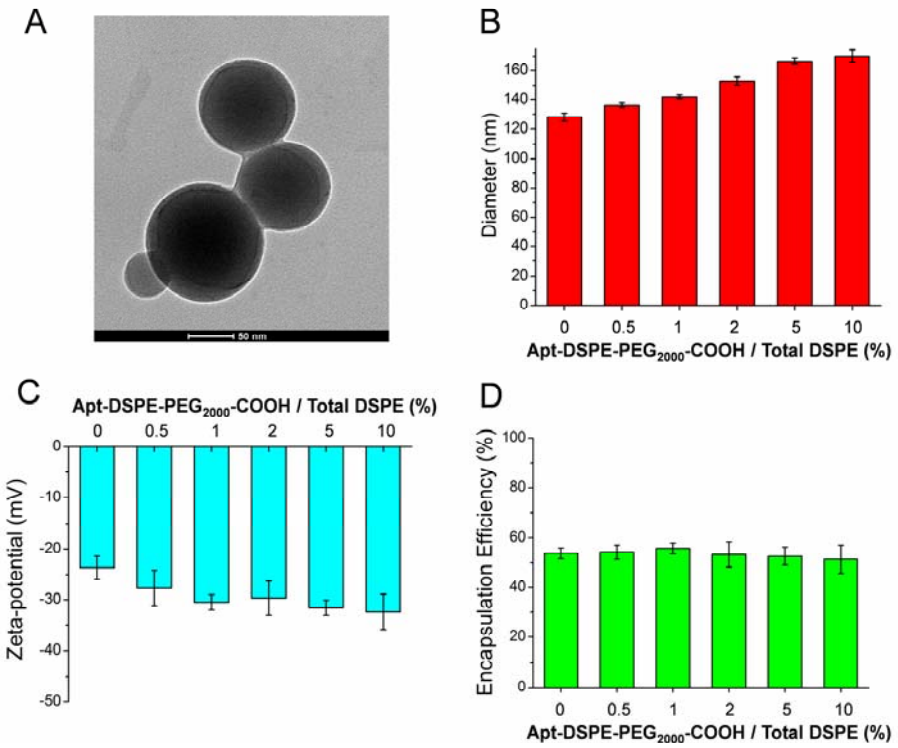

Figure 2. (A) Transmission electron microscope (TEM) of Apt-VRL-NPs. The (B) diameter (C) zeta-potential and (D) encapsulation efficiency of NPs with various aptamer densities. Data is shown as mean ± SD from three separate experiments.

***In vitro* drug releasing profile.** The *in vitro* VRL release from the NPs was investigated in PBS buffer at pH 7.4 (Figure 3A). The releasing rate was identical regardless of aptamer attachment ($P > 0.05$). The cumulative release has an initial burst in the first 2 h. Following the initial burst, the release was sustained over the next few days. After 72 h, the amount of VRL released reached ~35%. After that, the release was even slower, reaching the maximum release of ~38% in 108 h. This release profile is typical for many polymer-based carriers,[58] indicating the successful encapsulation of the drug in PLGA. The sustained release can decrease administering frequency and enhance patient compliance. In our previous study, the release profile of VRL from naked PLGA NPs (no lipid) was much faster, with nearly 45% released in the initial 20 h.[49] We attribute this difference to the lipid shell slowing down PLGA hydrolysis.

Since VRL is non-fluorescent, to track its delivery in cells, Coumarin-6 (Cou-6) labeled

NPs were also prepared. The size and surface charge of these NPs were almost identical to those loaded with VRL, except that the Cou-6 encapsulation efficiency was higher (~89%). Therefore, Apt_{10}-Cou-6-NPs (i.e. with 10% aptamer) were used as a model to study the *in vitro* behavior of these NPs. The release profile of Cou-6 was even slower. For both the aptamer-conjugated and aptamer-free NPs, only ~5% Cou-6 was released after 24 h (Figure 3B). Therefore, this dye molecule has a stronger interaction with PLGA and might be encapsulated in the core of the polymer particles. Since most of our cellular uptake experiments lasted only a few hours, the release of Cou-6 is minimal during this period. This makes it ideal for NP tracking.

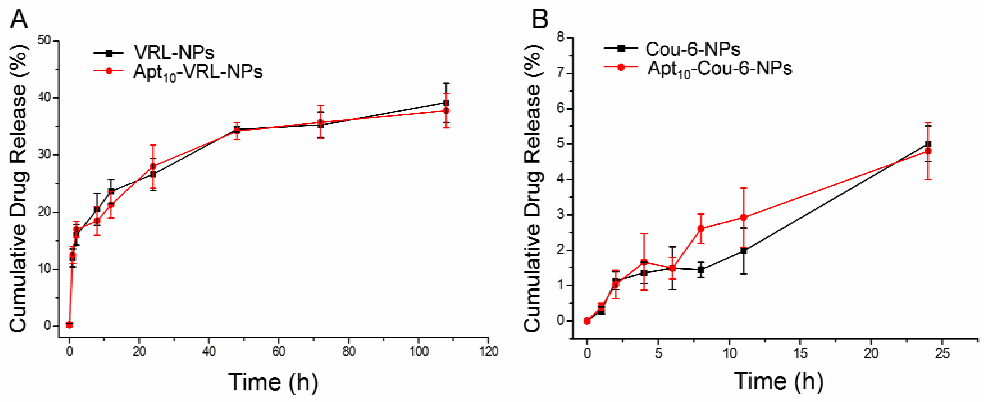

Figure 3. (A) *In vitro* release profile of VRL-NPs and Apt_{10}-VRL-NPs in PBS buffer (pH 7.4) using the membrane diffusion method. (B) *In vitro* release profile of Cou-6 loaded NPs. Data is represented as the mean ± SD of three separate experiments.

Cellular uptake. Because VRL is non-fluorescent, we cannot track the VRL in the cells. Therefore, we used the Cou-6 NP for tracking. After internalization by the cells, the NPs are expected to be destroyed by the endosomes and lysosomes, releasing Cou-6 into the cytoplasm. With this in mind, cellular uptake of Cou-6 loaded NPs was first evaluated by fluorescence microscopy. Two cell lines were studied and the cells were imaged in the green channel for Cou-6 and the blue channel for the nuclear stain. The merged images are shown in Figure 4. It can be observed that the fluorescence of Cou-6 in the cytoplasm is brighter than in the nucleus, indicating that most of the particles were internalized. If the NPs were

only adsorbed on the cell surface, the fluorescence would be stronger on the contour of the cells. Internalization of another mucin targeting aptamer by cells has been reported previously.[59] Cells can internalize NPs by endocytosis, which should be promoted by aptamer binding. Further evidence for internalization is from the subsequent toxicity studies (*vide infra*).

The HepG2 cells, without the overexpressed MUC1 protein, were used as a negative control. For the HepG2 cells, a similar uptake was observed for NPs without (Figure 4A) or with (Figure 4C) the aptamers. The MCF-7 cells overexpress the target protein on their surfaces. For the NPs without the aptamer, we also observed low fluorescence intensity (Figure 4B). The NPs with aptamer produced a significantly stronger fluorescence (Figure 4D), confirming the role of aptamer in assisting cellular uptake.

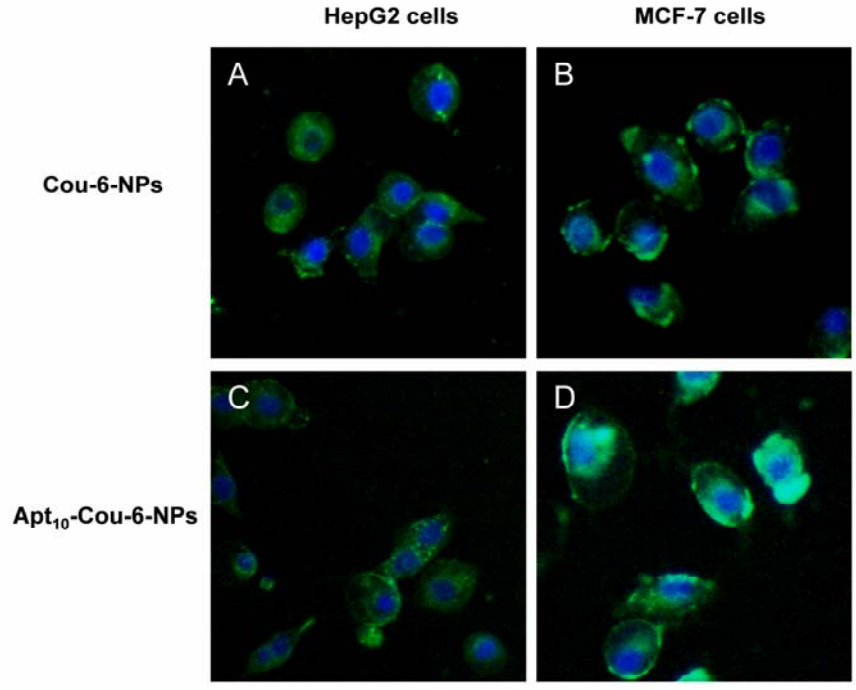

Figure 4. Microscopy images showing the internalization of Cou-6-NPs (A and B) and Apt_{10}-Cou-6-NPs (C and D) in HepG2 cells (A and C) and MCF-7 cells (B and D) after 30 min incubation. The green color shows the fluorescence from the Cou-6 dye. The blue color shows the fluorescence from the DAPI dye in the nuclei (magnification: 100×). The NP

concentrations were 100 µg/mL for this experiment.

The initial microscopy studies above supports the cellular accumulation of the aptamer-conjugated NPs. To quantitatively investigate cellular uptake, we further tested the effect of NP concentration using a microplate reader to measure the fluorescence in each well. Figure 5 indicates that for all of the formulations, cell uptake increased with increasing NP concentration. For the HepG2 cells, the difference between the two types of NPs was very small in all the tested concentrations (Figure 5A). For the MCF-7 cells (Figure 5B), on the other hand, the aptamer-functionalized NPs experienced more cellular uptake. For most of the experiments, a NP concentration of 100 µg/mL (calculated based on PLGA) was used.

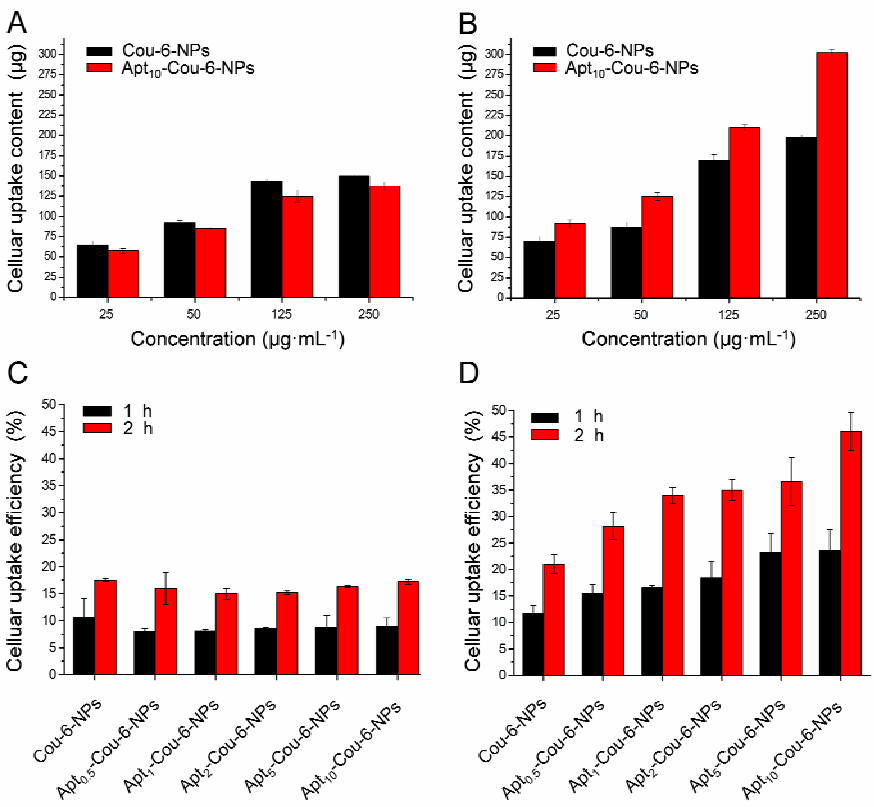

Figure 5. The influence of Cou-6-NPs concentration on cellular uptake by (A) HepG2 cell and (B) MCF-7 cells for the NPs with and without the aptamer attachment. The uptake efficiency of Cou-6-NPs and Apt-Cou-6-NPs by (C) HepG2 cell and (D) MCF-7 cell for 1 and 2 h. Data is shown as mean ± SD from three independent experiments.

Next, the effect of aptamer density and incubation time was compared (Figure 5C, D). For both cell lines, the uptake almost doubled with the increase of incubation time from 1 to 2 h, indicating time-dependent cellular uptake. The uptake efficiency barely changed for the HepG2 cells as a function of the aptamer density (Figure 5C). For the MCF-7 cells, a steady increase in uptake was observed as the aptamer density was increased (Figure 5D) which further confirmed the targeting ability of the aptamer.

The binding of the aptamer to the target protein is specific and strong (K_d = 0.135 nM).[41] By immobilizing multiple copies of the aptamers on each NP, the apparent affinity should be even stronger. In this work, a series of aptamer concentrations (0, 0.225, 0.45, 0.9, 2.25, 4.5 nmol) for each mg of PLGA were tested. If all the added aptamers were conjugated, the number of aptamer molecules on each NP was calculated to be 173 for the 0.5% aptamer formulation and 3465 for the 10% formulation. We showed that even $Apt_{0.5}$-Cou-6-NPs, with the lowest aptamer density, were able to target MUC1 cells and be internalized. When incubated with MCF-7 cells for 2 h, the uptake of $Apt_{0.5}$-Cou-6-NPs was 2.2 fold greater than with Cou-6-NPs. Increased aptamer density may promote a better binding avidity due to polyvalent interactions.[6,57,60] Our work herein indicates that the S2.2 aptamer can achieve the polyvalent effect as well.

Cell growth inhibition. To understand the efficacy of this delivery vehicle, VRL-loaded NPs were tested against both cell lines using the MTT assay. The cells were respectively treated with the plain NPs, the free aptamer, free VRL, and VRL-loaded NPs with various aptamer densities (Figure 6A). The plain NPs and free aptamer showed almost no toxicity to both cell lines after 24 h incubation, which is consistent with the high biocompatibility of these materials (e.g. PLGA, lipid, and DNA). VRL is poorly soluble in aqueous media, which might have limited its toxicity. The inhibition ratio of the free drug (12 μg/mL) to HepG2 and MCF-7 cells was 25.0% and 26.8%, indicating the drug has similar cancer killing efficiency in both of these cells. Free VRL can enter cells through passive diffusion.

VRL loaded NPs showed similar toxicity compared to free VRL for the HepG2 cells

(black bars, $P<0.05$), while their toxicity to the MCF-7 cells increased with increasing aptamer density (red bars). At the highest aptamer density, the toxicity reached 1.7-fold compared the aptamer-free formulation. The targeted delivery system has enhanced cellular uptake, based on the above fluorescence studies, explaining the increased toxicity.

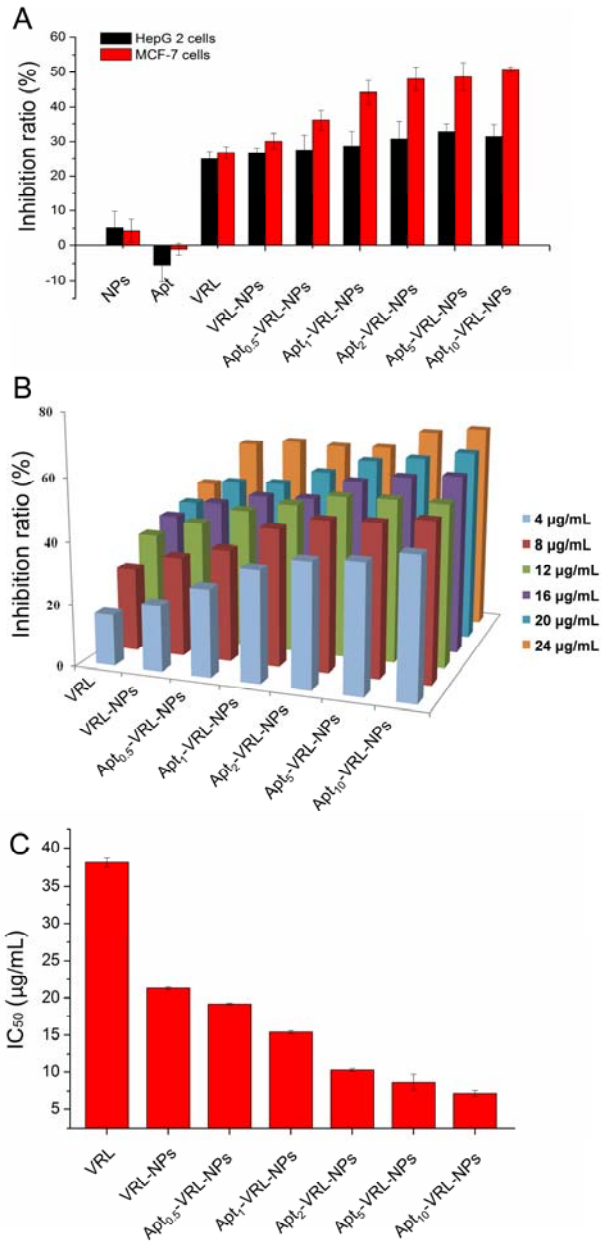

Figure 6. (A) Cytotoxicity of various reagents on HepG2 cells and MCF-7 cells treated for 4 h with plain NPs, free VRL, free aptamer, VRL-NPs and Apt-VRL-NPs. (B) Inhibition of MCF-7 cells exposed to VRL, VRL-NPs and Apt-VRL-NPs. (C) IC_{50} values of VRL, VRL-NPs and Apt-VRL-NPs on MCF-7 cells. Data is shown as mean ± SD of four

independent experiments.

Next the VRL concentration was varied (Figure 6B). We found that the aptamer made the largest difference in efficacy at low drug concentrations. For example, with only 4 $\mu g \cdot mL^{-1}$ of VRL, the cell inhibition was only 16.6% for the free drug. The inhibition increased to 21.3% for VRL loaded into the NPs without the aptamer. With the highest aptamer density, the toxicity increased to over 40%. Figure 6C shows the IC_{50} of each aptamer modified NP. Compared to the free VRL (IC_{50} = 38 μg/mL), the formulation with the highest aptamer density has an IC_{50} value of 7.2 μg/mL (P<0.05). Therefore, the aptamer has increased the efficacy of the drug by more than 5-fold. Moreover, from the results of the MTT experiment, the IC_{50} value is dose-dependent. We reason that the VRL released from the NPs has entered the cell nucleus to execute its function on microtubules.

Conclusions

In this work, anticancer drug VRL loaded lipid-polymer hybrid NPs were constructed and functionalized with the S2.2 aptamer for targeting the MUC1 protein overexpressed tumor cells (MCF-7). This NP formulation has a high drug encapsulation efficiency and sustained drug release profile. The aptamer-functionalized NPs showed good efficacy on MCF-7 cells. More importantly, the targeting capability and cell inhibition ratio improved with an increased S2.2 aptamer density on the surface. All of these results indicate that these lipid coated polymer NPs with aptamer targeting ligands are a promising anticancer drug delivery system.

Acknowledgements

This work was supported by the Shenghua Scholar Foundation, the Postdoctoral Science Foundation of Central South University and China (Grant No. 124896), and the International Postdoctoral Exchange Fellowship Program [2014]29 (Grant No. 20140014).

References

1. Y. C. Tseng, S. Mozumdar and L. Huang, *Adv. Drug Deliver. Rev.*, 2009, **61**, 721.
2. T. M. Allen and P. R. Cullis, *Adv. Drug Deliver. Rev.*, 2013, **65**, 36.
3. Y. Malam, M. Loizidou and A. M. Seifalian, *Trends Pharmacol.Sci.*, 2009, **30**, 592.
4. W. T. Al-Jamal and K. Kostarelos, *Acc. Chem. Res.*, 2011, **44**, 1094.
5. A. Samad, Y. Sultana and M. Aqil, *Curr. Drug Deliv.*, 2007, **4**, 297.
6. C. E. Ashley, E. C. Carnes, G. K. Phillips, D. Padilla, P. N. Durfee, P. A. Brown, T. N. Hanna, J. Liu, B. Phillips, M. B. Carter, N. J. Carroll, X. Jiang, D. R. Dunphy, C. L. Willman, D. N. Petsev, D. G. Evans, A. N. Parikh, B. Chackerian, W. Wharton, D. S. Peabody and C. J. Brinker, *Nat. Mater.*, 2011, **10**, 389.
7. J. Liu, A. Stace-Naughton, X. Jiang and C. J. Brinker, *J. Am. Chem. Soc.*, 2009, **131**, 1354.
8. S. Tan, X. Li, Y. Guo and Z. Zhang, *Nanoscale*, 2012, **5**, 860.
9. W. Gao, C. M. J. Hu, R. H. Fang and L. Zhang, *J. Mater. Chem. B*, 2013, **1**, 6569.
10. A. Verma and F. Stellacci, *Small*, 2010, **6**, 12.
11. R. C. Van Lehn, P. U. Atukorale, R. P. Carney, Y.-S. Yang, F. Stellacci, D. J. Irvine and A. Alexander-Katz, *Nano Lett.*, 2013, **13**, 4060.
12. P. C. Li, D. Li, L. X. Zhang, G. P. Li and E. K. Wang, *Biomaterials*, 2008, **29**, 3617.
13. J. M. Chan, L. Zhang, K. P. Yuet, G. Liao, J.-W. Rhee, R. Langer and O. C. Farokhzad, *Biomaterials*, 2009, **30**, 1627.
14. J. M. Chan, J.-W. Rhee, C. L. Drum, R. T. Bronson, G. Golomb, R. Langer and O. C. Farokhzad, *Proc. Natl. Acad. Sci. U.S.A.*, 2011, **108**, 19347.

15. Y. Liu, J. Pan and S.-S. Feng, *Int. J. Pharmaceut.*, 2010, **395**, 243.

16. A. Aravind, P. Jeyamohan, R. Nair, S. Veeranarayanan, Y. Nagaoka, Y. Yoshida, T. Maekawa and D. S. Kumar, *Biotechnol.Bioeng.*, 2012, **109**, 2920.

17. P. Zou, S. T. Stern and D. X. Sun, *Pharmaceutical Research*, 2014, **31**, 684.

18. X. R. Wen, K. Wang, Z. M. Zhao, Y. F. Zhang, T. T. Sun, F. Zhang, J. Wu, Y. Y. Fu, Y. Du, L. Zhang, Y. Sun, Y. H. Liu, K. Ma, H. Z. Liu and Y. J. Song, *PLoS ONE*, 2014, **9**, e106652.

19. L. F. Zhang, J. M. Chan, F. X. Gu, J. W. Rhee, A. Z. Wang, A. F. Radovic-Moreno, F. Alexis, R. Langer and O. C. Farokhzad, *ACS Nano*, 2008, **2**, 1696.

20. R. H. Fang, S. Aryal, C.-M. J. Hu and L. Zhang, *Langmuir*, 2010, **26**, 16958.

21. K. Hadinoto, A. Sundaresan and W. S. Cheow, *Eur. J. Pharm. Biopharm.*, 2013, **85**, 427.

22. B. Mandal, H. Bhattacharjee, N. Mittal, H. Sah, P. Balabathula, L. A. Thoma and G. C. Wood, *Nanomedicine: Nanotechnology, Biology and Medicine*, 2013, **9**, 474.

23. W. S. Cheow and K. Hadinoto, *Colloids Surf., B*, 2011, **85**, 214.

24. A. M. Scott, J. D. Wolchok and L. J. Old, *Nat Rev Cancer*, 2012, **12**, 278.

25. X. Zhao, H. Li and R. J. Lee, *Expert Opinion on Drug Delivery*, 2008, **5**, 309.

26. D. Peer, J. M. Karp, S. Hong, O. C. FaroKhzad, R. Margalit and R. Langer, *Nat. Nanotechnol.*, 2007, **2**, 751.

27. C.-M. J. Hu, S. Kaushal, H. S. T. Cao, S. Aryal, M. Sartor, S. Esener, M. Bouvet and L. Zhang, *Molecular Pharmaceutics*, 2010, **7**, 914.

28. Y. Liu, K. Li, B. Liu and S.-S. Feng, *Biomaterials*, 2010, **31**, 9145.

29. H. Wang, P. Zhao, X. Liang, X. Gong, T. Song, R. Niu and J. Chang, *Biomaterials*, 2010, **31**, 4129.

30. P. Zhao, H. Wang, M. Yu, S. Cao, F. Zhang, J. Chang and R. Niu, *Pharmaceutical Research*, 2010, **27**, 1914.

31. F. Huang, M. You, T. Chen, G. Zhu, H. Liang and W. Tan, *Chem. Commun.*, 2014, **50**, 3103.

32. X. H. Fang and W. H. Tan, *Acc. Chem. Res.*, 2010, **43**, 48.

33. D. Shangguan, Y. Li, Z. Tang, Z. C. Cao, H. W. Chen, P. Mallikaratchy, K. Sefah, C. J. Yang and W. Tan, *Proc. Natl. Acad. Sci. U.S.A.*, 2006, **103**, 11838.

34. M. S. L. Raddatz, A. Dolf, E. Endl, P. Knolle, M. Famulok and G. Mayer, *Angew. Chem. Int. Ed.*, 2008, **47**, 5190.

35. Y. F. Zhang, Y. Chen, D. Han, I. Ocsoy and W. H. Tan, *Bioanalysis*, 2010, **2**, 907-918.

36. D. H. J. Bunka and P. G. Stockley, *Nat. Rev. Microbiol.*, 2006, **4**, 588.

37. M. Famulok, J. S. Hartig and G. Mayer, *Chem. Rev.*, 2007, **107**, 3715.

38. Z. H. Cao, R. Tong, A. Mishra, W. C. Xu, G. C. L. Wong, J. J. Cheng and Y. Lu, *Angew. Chem. Int. Ed.*, 2009, **48**, 6494.

39. T. Chen, M. I. Shukoor, Y. Chen, Q. Yuan, Z. Zhu, Z. Zhao, B. Gulbakan and W. Tan, *Nanoscale*, 2011, **3**, 546.

40. Y. Wu, K. Sefah, H. Liu, R. Wang and W. Tan, *Proc. Natl. Acad. Sci. U.S.A.*, 2010, **107**, 5.

41. C. S. M. Ferreira, C. S. Matthews and S. Missailidis, *Tumor Biol.*, 2006, **27**, 289.

42. C. Yu, Y. Hu, J. Duan, W. Yuan, C. Wang, H. Xu and X. D. Yang, *PLoS One*, 2011, **6**,

e24077.

43. P. Wu, Y. Gao, H. Zhang and C. Cai, *Anal Chem*, 2012, **84**, 7692.

44. Y. Hu, J. Duan, Q. Zhan, F. Wang, X. Lu and X. D. Yang, *PLoS One*, 2012, **7**, e31970.

45. L. Tan, K. G. Neoh, E. T. Kang, W. S. Choe and X. Su, *Macromol Biosci*, 2011, **11**, 1331.

46. M. Sonobe, K. I. Okubo, S. Teramukai, K. Yanagihara, M. Sato, T. Sato, F. Chen, K. Sato, T. Fujinaga, T. Shoji, M. Omasa, H. Sakai, R. Miyahara, T. Bando and H. Date, *Cancer Chemother Pharmacol*, 2014, **74**, 1199.

47. A. Chan, C. Shannon, R. de Boer, S. Baron-Hay, A. Redfern, A. Bauwens, P. Craft, S. Webb, A. Townsend and D. Kotasek, *Asia Pac J Clin Oncol*, 2014, **10**, 368.

48. J. You, F. Wan, F. de Cui, Y. Sun, Y. Z. Du and F. Q. Hu, *Int J Pharm*, 2007, **343**, 270.

49. W. Zhou, Y. Zhou, J. Wu, Z. Liu, H. Zhao, J. Liu and J. Ding, *J Drug Target*, 2014, **22**, 57.

50. R. H. Fang, S. Aryal, C. M. Hu and L. Zhang, *Langmuir*, 2010, **26**, 16958.

51. O. C. Farokhzad, S. Jon, A. Khademhosseini, T. N. Tran, D. A. Lavan and R. Langer, *Cancer Res*, 2004, **64**, 7668.

52. E. Kajiwara, K. Kawano, Y. Hattori, M. Fukushima, K. Hayashi and Y. Maitani, *J Control Release*, 2007, **120**, 104.

53. F. Wan, J. You, Y. Sun, X. G. Zhang, F. D. Cui, Y. Z. Du, H. Yuan and F. Q. Hu, *Int J Pharm*, 2008, **359**, 104.

54. D. C. Drummond, C. O. Noble, Z. Guo, M. E. Hayes, J. W. Park, C. J. Ou, Y. L. Tseng, K. Hong and D. B. Kirpotin, *J Pharmacol Exp Ther*, 2009, **328**, 321.

55. J. Wang, X. Xing, X. Fang, C. Zhou, F. Huang, Z. Wu, J. Lou and W. Liang, *Philos Trans A Math Phys Eng Sci*, 2013, **371**, 20120309.

56. S. Dhar, F. X. Gu, R. Langer, O. C. Farokhzad and S. J. Lippard, *Proc Natl Acad Sci U S A*, 2008, **105**, 17356.

57. F. Gu, L. Zhang, B. A. Teply, N. Mann, A. Wang, A. F. Radovic-Moreno, R. Langer and O. C. Farokhzad, *Proc. Natl. Acad. Sci. U.S.A.*, 2008, **105**, 2586.

58. A. Mukerjee and J. K. Vishwanatha, *Anticancer Research*, 2009, **29**, 3867.

59. C. S. M Ferreira, M. C. Cheung, S. Missailidis, S. Bisland, J. Gariepy. *Nucleic Acids Res.*, 2009, **37**, 866-76.

60. Y. F. Huang, H. T. Chang and W. Tan, *Anal. Chem.*, 2008, **80**, 567.